A NOVEL HAPTIC INTERFACE FOR EXTENDED RANGE TELEPRESENCE: CONTROL AND EVALUATION

Antonia Pérez Arias and Uwe D. Hanebeck
Intelligent Sensor-Actuator-Systems Laboratory (ISAS)
Institute for Anthropomatics
Universität Karlsruhe (TH), Germany
Email: aperez@ira.uka.de and uwe.hanebeck@ieee.org

Keywords: Extended range telepresence, motion compression, haptic interface, force control

Abstract: A novel haptic interface for extended range telepresence is presented that allows the user simultaneous wide area motion and haptic interaction in remote environments. To achieve an extended workspace, the haptic interface consists of a haptic manipulator for precise haptic rendering and a large portal carrier system that enlarges the workspace by prepositioning the end-effector. As the prepositioning unit is grounded and driven by three linear drives, our approach has the advantages of high force capability and an accurate positioning of the haptic interface. The use of this haptic interface with Motion Compression permits to explore large remote environments even from small user environments. As a result, not only has the user visual, acoustic, and haptic feedback, but can also control the teleoperator or avatar by natural walking, which considerably increases the sense of immersion. A prototype system for haptic extended range telepresence was designed, implemented, and tested.

1 INTRODUCTION

Telepresence aims at creating the impression of being present in an environment, which is inaccessible to a human user. Such an environment can be real or virtual, and will be referred to in the following as *target environment*. The feeling of presence is achieved by visual and acoustic sensory information recorded from the target environment and presented to the user on an immersive display.

The more of the user's senses are involved, the better the immersion in the target environment. In order to use the sense of motion as well, which is especially important for human navigation and way finding, the user's motion can be tracked and transferred to the *teleoperator*, a mobile robot or an avatar, in the target environment. As a result, in extended range telepresence the user can additionally use the proprioception, the sense of motion, to navigate the teleoperator by natural walking, instead of using devices like joysticks, pedals or steering wheels.

However, without further processing the motion information, the motion of the user is restricted to the size of the *user environment*, which is limited, for example by the range of the tracking system or the available space. *Motion Compression* (Nitzsche et al., 2004) is an algorithmic approach that provides a nonlinear transformation, mapping the path in the target environment to a feasible path in the user environment by minimizing proprioceptive and visual inconsistencies.

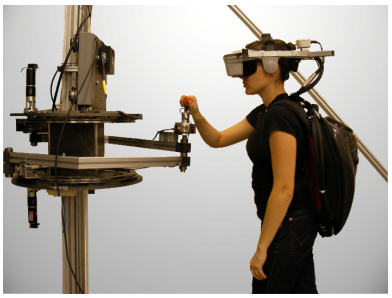

Figure 1: User and haptic interface for interaction with extended target environments.

Extended range telepresence can be applied in many fields, especially in those that require the human navigation skills to solve the task, for example tele-

exploration of remote environments, visualization of complex structures, training of emergency evacuations, etc. An extended range telepresence system that uses Motion Compression to teleoperate a mobile robot is presented in (Rößler et al., 2005). Since haptic information is indispensable, amongst others, for haptic exploration and manipulation of objects in the target environment, a novel haptic interface for the extended range telepresence system was built. A picture of the system is shown in Fig. 1.

Force reflecting telepresence systems usually assume an immobile user and a restricted workspace. For example, industrial robots have often been used as haptic interfaces due to their accuracy and relative high force capability (Hoogen and Schmidt, 2001) but their limited workspace makes them unfeasible for extended range telepresence. In the last years, several haptic interfaces that allow a dexterous feedback and fairly high forces have been designed to enlarge their workspaces, e.g. a string-based haptic interface (Bouguila et al., 2000), or a grounded hyper-redundant haptic interface in (Ueberle et al., 2003). Portable haptic interfaces like exoskeletons (Bergamasco et al., 1994) solve the problem of wide area motion, since the interface is carried along by the user. However, working with exoskeletons can be fatiguing for the user due to the high weight of the system. In addition, they can display lower forces than grounded displays (Richard and Cutkosky, 1997). The only group of systems that really allow haptic interaction during wide area motion are mobile haptic interfaces (Nitzsche et al., 2003), (Formaglio et al., 2005), (Peer et al., 2007). These are usually small haptic devices mounted on a mobile platform. Drawbacks of such interfaces are a difficult control and a dependency of the force display quality on the localization of the mobile platform.

In this paper, we present a novel haptic device that allows haptic interaction in extended range telepresence and combines the advantages of grounded and mobile haptic interfaces. It consists of a grounded linear prepositioning unit that moves along with the user and a manipulator arm attached to the prepositioning unit that is used to display forces at any position in the user environment. This haptic interface allows in conjunction with Motion Compression unrestricted wide area motion and the possibility of effectively guiding the user in the target environment by means of haptic information. The control of the haptic interface is based on the decoupling of force control and prepositioning of the haptic device, which takes both the optimal manipulator's configuration and the user's position into consideration.

The remainder of this paper proceeds as follows. The following section presents the extended range telepresence system. Motion Compression is reviewed, since it determines the requirements of the haptic interface, and the mechanical setup of the haptic interface is presented. In section 3, a detailed description of the control design is given. Experimental results are shown in section 4. Finally, a summary and an outlook can be found in section 5.

2 EXTENDED RANGE TELEPRESENCE SYSTEM

2.1 Motion Compression

Motion Compression provides a nonlinear mapping between the user's path in the user environment and the path in the target environment. It consists of three modules: *Path prediction* tries to predict the desired path of the user in the target environment by means of tracking data and, if possible, information of the target environment. The resulting path is called *target path*. *Path transformation* transforms the target path so that it fits in the user environment. The resulting *user path* conserves the length and turning angles of the target path while there is a minimum difference in curvature. Fig. 2 shows these paths in both environments. Finally, the *user guidance* module guides the user on the user path, while he has the impression of walking on the original target path.

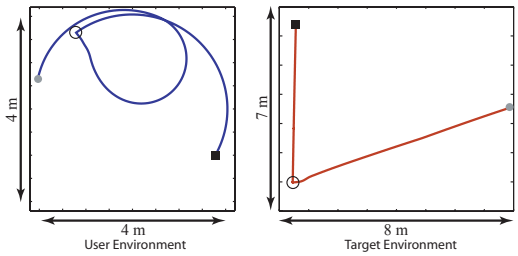

Figure 2: The corresponding paths in both environments. Left: user path in the user environment. Right: target path in the target environment.

The result of Motion Compression is a transformation between the user's position in the user environment and the teleoperator's position in the target environment at any time and position. This transformation can also be used to map the user's hand position, or to transform force vectors recorded by the teleoperator back into the user environment.

The use of Motion Compression for extended range telepresence puts a number of demands on the design of a haptic interface. The haptic interface must

be able to reach all configurations in a user environment of $4 \times 4\,\mathrm{m}^2$, in which the user may move with a natural speed of up to $2\,\mathrm{m/s}$. Especially the rotational motion around the vertical axes must be unlimited.

2.2 A Novel Haptic Interface: Setup

Fine haptic rendering and wide area motion require very different characteristics regarding mechanics as well as control. Therefore a novel haptic interface was designed that consists of two subsystems: a linear prepositioning unit that accompanies the user along the user path so that he does not perceive the haptic display, and a manipulator arm attached to the prepositioning unit that is used to display defined forces at any position in the user environment. In this way, the workspace of the haptic interface covers the whole user environment. Fig.3 shows a CAD drawing of the complete setup.

The motion subsystem is realized as grounded portal carrier system of approximately $5 \times 5 \times 2\,\mathrm{m}^3$ with three translational degrees of freedom, which are realized by three independent linear drives. These linear drives are built using a commercially available carriage-on-rail system. The carriages are driven by a toothed belt. The x- and y-axis consist of two parallel rails each for stability reasons, while the z-axis is only a single rail. As a result, the system is driven by five synchronous AC-motors with helical-bevel servo gear units of 120 Nm maximal torque, that allow a maximum speed of $2\,\mathrm{m/s}$ and an acceleration of $2\,\mathrm{m/s}^2$. As the configuration space equals cartesian space, forward kinematics can be expressed by means of an identity matrix. Thus position control is extremely easy to handle and very robust (Rößler et al., 2006).

This construction has the advantages of a a high force capability and an accurate positioning of the manipulator, which is determined directly through encoder's information with relative accuracy 0.1 mm. By using a position control with high gains, the user does not perceive the motion subsystem, and the transparency depends only on the force-controlled subsystem (Nitzsche et al., 2003).

Because the acceleration of the human hand is typically much higher than the acceleration of the portal carrier, a fast manipulator was used. It covers the human arm workspace and has planar movement. It is implemented as a planar SCARA arm, which is attached to the z-axis of the portal carrier. The redundant planar degrees of freedom permit the separation of positioning and force display. Two active rotational joints driven by two 150 W DC-motors are integrated into the base, so that all moving joints are passive. Circular drives allow infinite motion around the z-axis. The manipulator arm was designed to display a force of 50 N at the end-effector. More details can be found in (Rößler et al., 2006).

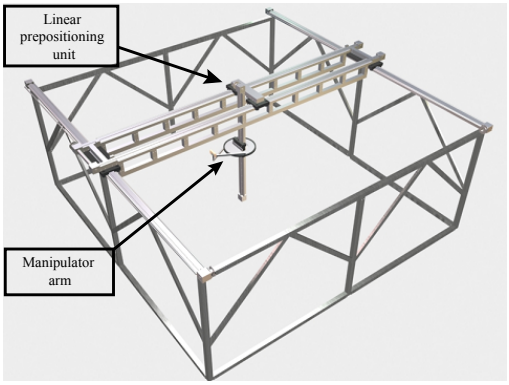

Figure 3: CAD drawing of the complete setup with linear positioning unit and manipulator arm.

3 CONTROL DESIGN OF THE HAPTIC INTERFACE

3.1 Kinematic Model

The control of this haptic interface is based on the decoupling of force control at the end-effector and position control of the haptic device. The position of the end-effector with respect to the basis coordinate frame $\underline{x}_E$ is described by the global position of the linear prepositioning unit, $\underline{x}_L$, and $\underline{x}_S$, the relative position of the manipulator arm with respect to the linear prepositioning unit as $\underline{x}_E = \underline{x}_L + \underline{x}_S$.

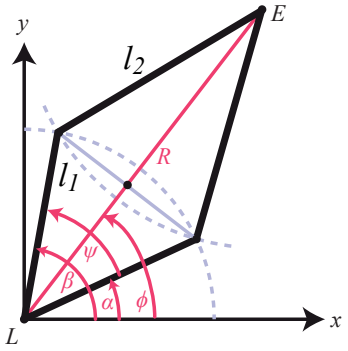

Figure 4: Geometrical SCARA-Model.

Fig. 4 shows the geometrical SCARA-model used to derive the kinematic equations. L represents the linear prepositioning unit, E the end-effector, and l_1

and l_2 the lengths of the inner and outer segments, respectively. If only the joints at the angles α and β are actively driven, the end-effector position $\underline{x}_E$ can be expressed as

$$\underline{x}_E = \underline{x}_L + \underline{x}_S = \begin{bmatrix} x_L \\ y_L \end{bmatrix} + \begin{bmatrix} \cos\left(\frac{\alpha+\beta}{2}\right) \cdot R \\ \sin\left(\frac{\alpha+\beta}{2}\right) \cdot R \end{bmatrix}, \quad (1)$$

where R, the radial travel, is calculated as

$$R = l_1 \cos\left(\frac{\beta-\alpha}{2}\right) + \sqrt{l_2^2 - l_1^2 \sin^2\left(\frac{\beta-\alpha}{2}\right)} \quad (2)$$

With this equation the direct kinematics of the manipulator is defined. The Jacobian of the manipulator $J(\gamma)$ on the configuration space $\gamma = \begin{bmatrix}\alpha & \beta\end{bmatrix}^{\mathrm{T}}$, which will be used next for the control of the haptic interface, is defined as

$$J\left(\underline{\gamma}\right) = \frac{\partial \underline{x}_S\left(\underline{\gamma}\right)}{\partial \underline{\gamma}} \quad (3)$$

3.2 Control Structure

Fig. 5 illustrates the block diagram of the control scheme with force feedback, as well as the position control of the haptic display. The end-effector velocity of the haptic interface $\underline{\dot{x}}_E$ is transmitted via the communication channel and acts as reference velocity at the end-effector of the teleoperator $\underline{\dot{x}}_{E,ref,T}$. The environment reacts according to its impedance with a reaction $\underline{F}_T$, which is measured by the teleoperator, and transmitted to the haptic interface as reference input $\underline{F}_{T,ref,U}$. This architecture represents a two-channel force-velocity bilateral control.

In our system, the haptic interface is modelled as an admittance, which transforms $\underline{F}_{U,ref}$, the reference force to be displayed, into the reference motion of the end-effector as

$$\underline{F}_{U,ref} = M \cdot \underline{\ddot{x}}_{E,ref} + D \cdot \underline{\dot{x}}_{E,ref}, \quad (4)$$

where M is the desired mass matrix and D the desired damping matrix. The admittance control scheme is very well suited for systems with nonlinearities and large dynamic properties because the admittance model shapes the desired dynamic behaviour of the system by compensating the natural device dynamics (Ueberle and Buss, 2004).

The resolved acceleration control (J^{-1} *control*) is applied to calculate the commanded motor torque of the manipulator $\underline{\tau}_{ref}$:

$$\underline{\tau}_{ref} = \hat{M} \cdot J^{-1} \cdot \underline{\ddot{x}}_C + \underline{h}\left(\underline{\gamma}, \underline{\dot{\gamma}}\right) \cdot \underline{\dot{\gamma}} + \underline{g}\left(\underline{\gamma}\right), \quad (5)$$

where $\hat{M}$ is an approximation of the device joint inertia matrix and J is the Jacobian. The vectors $\underline{h}$, representing the friction effects, and $\underline{g}$ can be approximated through experimental identification.

The user, while moving the end-effector, applies a force consisting of a voluntarily applied force and a reaction force induced by the arm impedance. In order to reconstruct the applied force from the measured force $\underline{F}_U^*$ and the velocity of the end-effector, a model of the human arm impedance is applied:

$$\underline{F}_U = \underline{F}_U^* + M_u \cdot \underline{\ddot{x}}_E + D_u \cdot \underline{\dot{x}}_E + K_u \cdot \underline{x}_E \quad (6)$$

It is known that the arm impedance varies with the user and the arm configuration. Hence, the mean values of multiple users and planar configurations were used: $M_u = 2\,\mathrm{Kg}$, $D_u = 6\,\mathrm{Ns/m}$, and $K_u = 10\,\mathrm{N/m}$.

The reference position of the linear prepositioning unit $\underline{x}_{L,ref}$, which can be easily controlled in cartesian coordinates, is calculated by optimizing the manipulator's configuration according to some performance measure.

3.3 Prepositioning

When attaching the SCARA manipulator to the portal carrier, there is a redundancy in the planar directions that may be resolved by optimizing the manipulability of the SCARA. The manipulability is usually represented as

$$w\left(\underline{\gamma}\right) = \sqrt{det\left(J^T(\underline{\gamma}) \cdot J(\underline{\gamma})\right)}. \quad (7)$$

For $l_1 = 0.285\,\mathrm{m}$ and $l_2 = 0.708\,\mathrm{m}$, the SCARA robot's manipulability was found to be optimal when $\psi = \beta - \alpha = 2.048$.

Let's consider the polar coordinates of the end-effector's position: $R = l_1 \cos\left(\frac{\psi}{2}\right) + \sqrt{l_2^2 - l_1^2 \sin^2\left(\frac{\psi}{2}\right)}$, and $\phi = \frac{\alpha+\beta}{2}$. Since the manipulability w is independent of ϕ, another criterion must be found to optimize this parameter. It is also crucial to avoid collisions with the user, therefore the angle ϕ is chosen that maximizes the distance d between the user and the prepositioning unit by adopting $R^{opt} = R\left(\psi^{opt}\right)$. By designating $\underline{x}_{EH}$ the vector from the end-effector's position to the user's position, and θ the angle between this vector and the x-axis, the distance d can be expressed as

$$d = R^{opt\,2} + |\underline{x}_{EH}|^2 - 2R\,|\underline{x}_{EH}| \cos(\theta - \phi + \pi), \quad (8)$$

and it is maximal when $\phi^{opt} = \theta$, or in other words, when the linear prepositioning unit is situated in front of the user, and lies on the connecting line between the user's head and the end-effector. The optimal joint

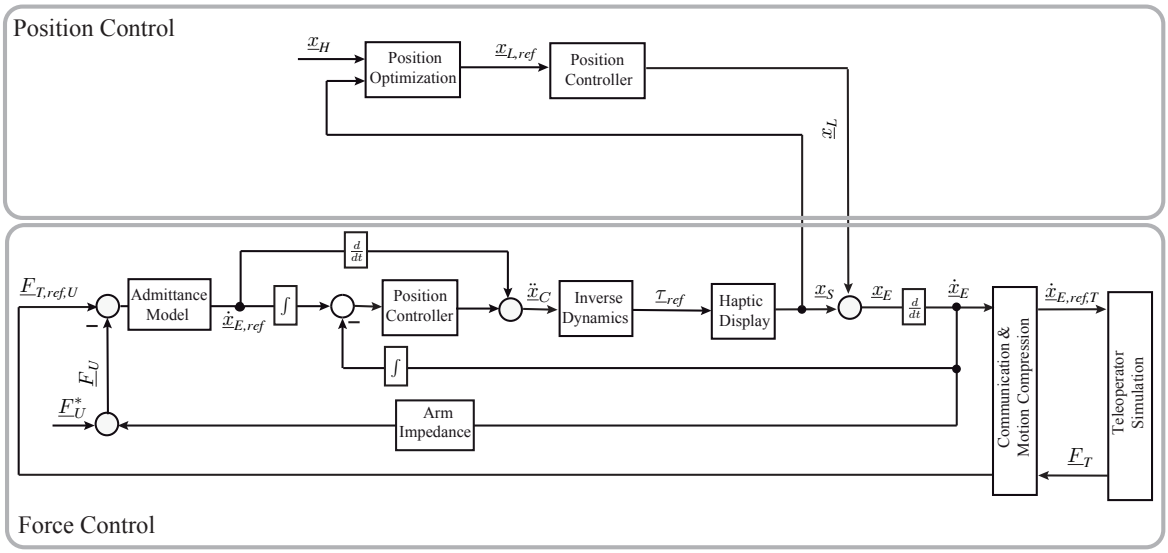

Figure 5: Control scheme of the haptic interface.

angles are finally $\alpha^{opt} = \phi^{opt} - \frac{\psi^{opt}}{2}$ and $\beta^{opt} = \phi^{opt} + \frac{\psi^{opt}}{2}$.

With $\underline{x}_S^{opt} = \left[\cos(\phi^{opt}) \cdot R^{opt} \quad \sin(\phi^{opt}) \cdot R^{opt}\right]^{\mathrm{T}}$ being the optimal configuration of the manipulator, the reference position of the linear prepositioning results $\underline{x}_{L,ref} = \underline{x}_E - \underline{x}_S^{opt}$.

4 EXPERIMENTS

Two kinds of experiments were performed in order to evaluate the proposed haptic interface. First, the proposed force control was tested and second, the simultaneous wide area motion with haptic interaction was validated.

The force at the end-effector, and the positions of both, end-effector and prepositioning unit, were recorded during free motion and during a hard contact. In order to achieve transparency, the reference force during free motion is $\underline{F}_{T,ref,U} = 0\,\mathrm{N}$. An admittance of $M = 4\,\mathrm{kg}$ was simulated. The control gains of the prepositioning and the admittance position controller were obtained experimentally using standard Ziegler-Nichols.

Fig. 6 shows the force-position plots for the x-direction, when a user walks 15 seconds back and forth about 2 m in x-direction. Analogously, Fig. 7 represents the reference and the measured force when a user walks against a wall at position $-0.5\,\mathrm{m}$ with rigidity $K = 700\,\mathrm{N/m}$. The maximal displayed force is limited to 60 N. Both figures also show the motion of the linear positioning unit at an optimal distance of the end-effector.

The main advantage of the admittance control is that the desired mass and damping of the device can be shaped. However, it is known that the admittance control reduces the force bandwidth of the haptic system.

The prepositioning was tested together with the haptic interaction to validate the entire concept of the haptic interface. For this purpose, the virtual and the user environment were supposed coincident, i.e. $4 \times 4\,\mathrm{m}^2$ large, and two virtual walls were placed inside. Fig. 8 shows the results of this experiment. The motion of the user can be divided into four segments: a) the user moves toward the wall, b) the user walks along the wall 1, c) the user walks along the wall 2, and d) the user turns on place. The haptic interface is always on the opposite side of the end-effector, so that the danger of a collision with the user is avoided. At the same time, the distance between the end-effector and the basis of the haptic interface is kept constant on the optimal value that maximizes the manipulability of the haptic display.

5 CONCLUSIONS

This paper presents a novel multi-modal telepresence system for extended range telepresence, which enables the user to explore remote environments by natural walking. To achieve this goal, a novel haptic interface was developed, which consists of a haptic manipulator mounted on a linear prepositioning unit that follows the user by keeping the optimal configu-

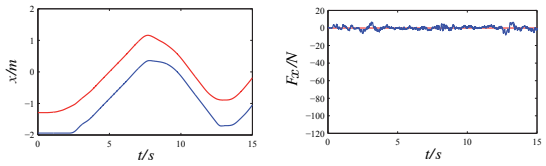

(a) (b)

Figure 6: Position and force during free motion. (a) End-effector position x_E (red), linear system position x_L (blue). (b) Reference force $F_{x,ref} = 0\,\mathrm{N}$ (red), actual force F_x (blue).

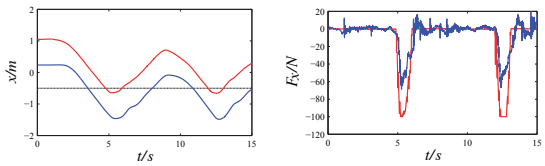

(a) (b)

Figure 7: Position and force by hard contact. (a) End-effector position x_E (red), linear system position x_L (blue). (b) Reference force $F_{x,ref}$ (red), actual force F_x (blue).

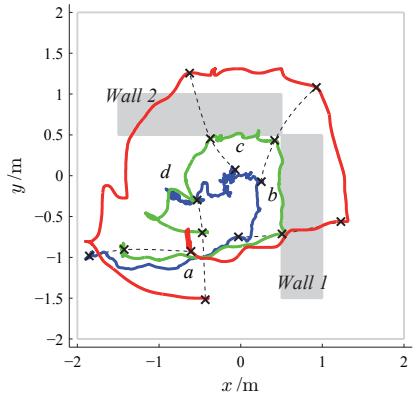

Figure 8: Positions of user x_H (blue), end-effector x_E (green) and linear system x_L (red) in presence of virtual walls during wide area motion.

ration of the manipulator and avoiding collisions with the user. For the haptic feedback, a dedicated force control was implemented and tested. It uses an admittance model to shape the dynamics of the system, as well as a model of the impedances of arm and manipulator to compensate their undesired dynamics. Experiments show the suitability of this haptic interface for extended range telepresence.

The use of haptic information in extended range telepresence to improve the user guidance is a promising application of the presented haptic interface, which is currently being investigated. For this application, the simultaneous compression of head and hand motion represents a further challenge.

REFERENCES

Bergamasco, M., Allotta, B., Bosio, L., Ferretti, L., Perrini, G., Prisco, G. M., Salsedo, F., and Sartini, G. (1994). "An arm exoskeleton system for teleoperation and virtual environment applications". In *Proceedings of the IEEE Intl. Conference on Robotics and Automation*.

Bouguila, L., Ishii, M., and Sato, M. (2000). "Multi-modal haptic device for large-scale virtual environment". In *Proceedings of the 8th ACM Intl. Conference on Multimedia*.

Formaglio, A., Giannitrapani, A., Barbagli, F., Franzini, M., and Prattichizzo, D. (2005). "Performance of mobile haptic interfaces". In *Proceedings of the 44th IEEE Conference on Decision and Control and the European Control Conference*.

Hoogen, J. and Schmidt, G. (2001). "Experimental results in control of an industrial robot used as a haptic interface". In *Proceedings of the IFAC Telematics Applications in Automation and Robotics*.

Nitzsche, N., Hanebeck, U. D., and Schmidt, G. (2003). "Design issues of mobile haptic interfaces". *Journal of Robotic Systems*, 20(9):549–556.

Nitzsche, N., Hanebeck, U. D., and Schmidt, G. (2004). "Motion compression for telepresent walking in large target environments". *Presence*, 13(1):44–60.

Peer, A., Komoguchi, Y., and Buss, M. (2007). " Towards a mobile haptic interface for bimanual manipulations". In *Proceedings of the IEEE/RSJ Intl. Conference on Intelligent Robots and Systems*.

Richard, C. and Cutkosky, M. R. (1997). "Contact force perception with an ungrounded haptic interface". In *Proceedings of ASME IMECE 6th Annual Symposium on Haptic Interfaces*.

Rößler, P., Armstrong, T., Hessel, O., Mende, M., and Hanebeck, U. D. (2006). "A novel haptic interface for free locomotion in extended range telepresence scenarios". In *Proceedings of the 3rd Intl. Conference on Informatics in Control, Automation and Robotics*.

Rößler, P., Beutler, F., Hanebeck, U. D., and Nitzsche, N. (2005). "Motion compression applied to guidance of a mobile teleoperator". In *Proceedings of the IEEE Intl. Conference on Intelligent Robots and Systems*.

Ueberle, M. and Buss, M. (2004). "Control of kinesthetic haptic interfaces". In *Proceedings of the IEEE/RSJ Intl. Conference on Intelligent Robots and Systems, Workshop on Touch and Haptics*.

Ueberle, M., Mock, N., and Buss, M. (2003). "Towards a hyper-redundant haptic display". In *Proceedings of the International Workshop on High-Fidelity Telepresence and Teleaction*.